POSITIVE ION TEMPERATURES ABOVE THE F-LAYER MAXIMUM*

R. L. F. BOYD AND W. J. RAITT†

The ion mass analyser on the UK–US satellite Ariel was a spherically symmetric energy spectrometer. The spectral lines may thus be interpreted not only in terms of ionic mass and concentration but also in terms of ion temperature.

Analysis of the data obtained has made available a picture of ion temperature variation with latitude above 400 km. The results show considerable scatter from day to day together with a marked rise in oxygen ion temperature with latitude.

INTRODUCTION

The determination of ion energy (and hence mass) spectrum by the ion probe on the satellite Ariel I (1962 –) provided good data on ion temperatures from 26 April, 1962 to 5 June, 1962. Some data of reduced quality is available until 26 September, 1962. Temperature is obtained from the width of the energy spectrum line for particles arriving at the probe. In principle the lines of hydrogen, helium or oxygen may all yield temperatures. The data presented in this paper all come from a study of the oxygen line which requires a concentration of oxygen greater than about 10^5 cm^{-3}. This implies that for the present study only altitudes below 600 Km. were useful and orbit orientation was such that in the period of this study (Days 117 to 140) this altitude range corresponds to values of local solar time within two hours of noon.

OUTLINE OF THE EXPERIMENT

The probe consisted of a 9 cm. diameter sphere mounted on the spin axis of the satellite. A fine grid 10 cm. in diameter was biassed negatively so as to keep ambient electrons from reaching the sphere, which was subjected to a positive voltage sweep. By constructing the system so that the angular momentum distribution of ions approaching the inner sphere was negligibly distorted by the presence of the grid it becomes valid to obtain the energy distribution of the ions by Druyvesteyn's[1] analysis. The required second derivative of the current voltage curve was obtained electronically and so telemetered.

If R is the kinetic energy of an ion moving with a velocity equal to that of the satellite and K is the energy corresponding to the most probable ion thermal velocity then for R≫K the form of the energy spectrum line is

$$f(E) = [2\pi^{\frac{1}{2}}(\text{K.R.})^{\frac{1}{2}}]^{-1} \exp \frac{-(E-R)^2}{4\,\text{K.R.}}$$

Thus the breadth of the energy spectrum line depends not only on the thermal energy of the ions but also on the velocity of the satellite. It is roughly Gaussian in form with a width at the $\frac{1}{e}$ points of $4(\text{K.R.})^{\frac{1}{2}}$. For monatomic oxygen R is about 5eV and K about 0.1eV so the line width is over 2 volts. While this broadening reduces the mass resolution it greatly eases the problem of determining the ion temperature.

Medicus[2] has obtained a more exact expression for the energy distribution of ions with a Maxwellian distribution arriving at a moving vehicle shown plotted in Fig. 1.

Analysis of the Ariel data has been carried out by fitting values computed from the approximate expression to the observed data.

*This paper was contributed to *Goddard Space Flight Center* under the joint United Kingdom–United States program which developed and launched the satellite Ariel I.

†Both authors are affiliated with the Department of Physics, University College, London, England.

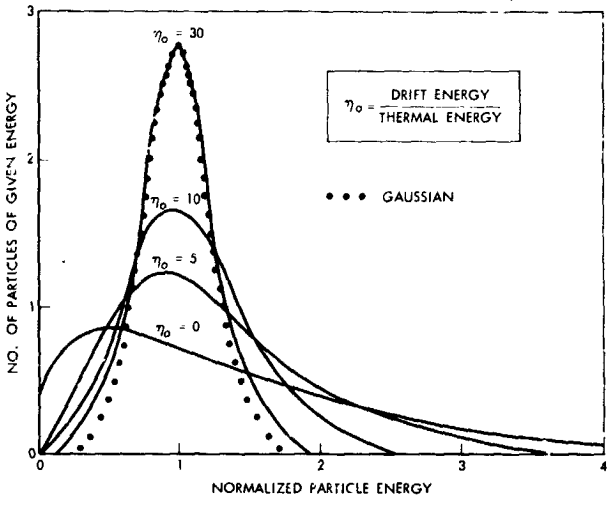

FIGURE 1.—Energy distribution of particles with Maxwellian distribution arriving at a moving vehicle.

EXPERIMENTAL RESULTS

The oxygen ion temperatures between 10 and 12 hours Local Solar Time measured in the longitude range −50° to 150° during the early northern summer of 1962 are plotted as a function of latitude in Fig. 2. The quantity of data is inadequate to make possible a complete decoupling of the effect of altitude from the effect of latitude. During the period selected, however, perigee was a little south of the equator so that the range of altitudes covered is not large. The approximate altitude corresponding to a given latitude is shown by the scale at the top of the figure.

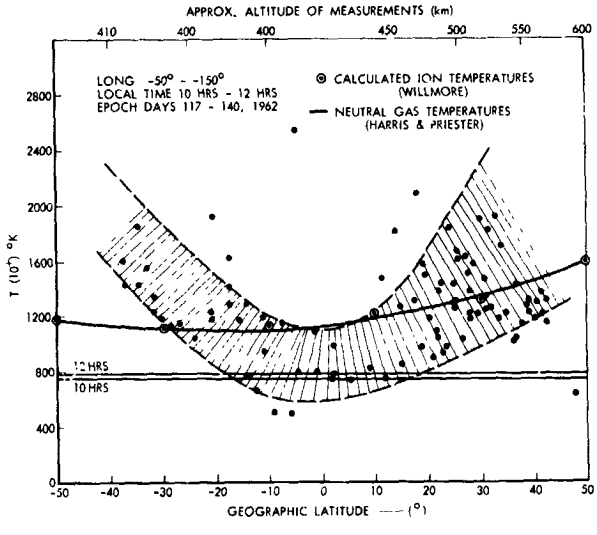

FIGURE 2.—Oxygen ion temperatures as a function of latitude.

Comparison of successive values of ion temperature obtained on a single pass suggest that instrumental consistency is at least as good as ±200 deg. K and possibly a good deal better. Most of the scatter of the points must therefore be taken to reflect real differences in ion temperature from one occasion to another.

Part of the scatter may be attributable to the range of local solar times, to the seasonal change and to the motion of the line of apsides. There may also be some dependence on magnetic activity and on longitude. However, it is not possible to account for most of the scatter in any of the above ways. The main conclusions are therefore that there is a variation in oxygen ion temperatures from one day to another amounting to several hundred degrees and that there is also a marked tendency of the oxygen ion temperatures to increase with latitude.

DISCUSSION OF RESULTS

Fig. 2 shows the neutral gas temperature based on the data of Harris and Priester[3] and a curve of ion temperature computed by A. P. Willmore[4] from the electron temperature data obtained on the same satellite (Willmore et al)[5] on the consideration that the heat flow from the electrons reaches the neutral gas by way of coulomb interaction with the ions. Willmore finds a rise of ion temperature with both latitude and altitude and appropriate weight has been given to both factors in plotting the curve from his data.

Except near the geomagnetic equator where the small dip angle would inhibit upward diffusion of photoelectrons, the energy input to the ionospheric electrons and hence to the ions due to solar radiation will vary as the cosine of the zenith angle.

Since the average fractional energy loss per collision of ions of mass M_i with gas atoms of mass M_g is

$$\frac{\Delta E}{3/2kT_i}=\frac{8}{3}\frac{M_iM_g}{(M_i+M_g)^2}\left(1-\frac{T_g}{T_i}\right)$$ where T_i and T_g refer to the ion and gas temperature.

We can write the energy flux

$$Q=4k\cdot n_i\cdot n_g\cdot S\cdot\left(\frac{3k}{2}\right)^{\frac{1}{2}}\left(\frac{T_i}{M_i}+\frac{T_g}{M_g}\right)^{\frac{1}{2}}\frac{M_iM_g}{(M_i+M_g)^2}(T_i-T_g)$$

where k is Boltzman's constant, n_i and n_g refer to the number densities of ions and gas atoms and S is the appropriate ion-atom energy exchange cross-section.

To a first approximation Q and n_i both vary as the cosine of the zenith $<$, n_g and T_g are constant and $(T_i - T_g) \ll T_g$. Thus writing $Q = Q \cos \chi$ and $n_i = n_0 \cos \chi$ we have

$$T_i - T_g \doteq Q_0 \left[4(3/2kT_g)^{\frac{1}{2}} \cdot n_0 \cdot n_g \cdot S \cdot k \cdot \left(\frac{1}{M_i} + \frac{1}{M_g} \right) \frac{M_i M_g}{(M_i + M_g)^2} \right]^{-1}$$

which shows that the factors most likely to influence the ion temperature in the topside ionosphere are ionic and neutral composition—affecting M_i, M_g and S—and ionic concentrations reduced to zero zenith angle, quantities which are also interrelated by the hydrostatic equation.

N_0 at the layer peak does in fact, fall with increasing latitude so the difference between the gas and ion temperature is to be expected to increase with latitude. The wide scatter in the data may well be related to variations not only in n_g but in ionic and possibly even in neutral particle composition. A preliminary consideration of the rate of energy exchange suggests that for the same flux the temperature difference between oxygen ions and helium atoms must be several times larger than when the ions are helium. The small amount of helium ion temperature data analysed so far supports this view. The possibility of the electric fields having an appreciable effect on the ion temperature would seem to be ruled out by the far larger effect they would have on the electrons.

One important factor must not be overlooked. It is the fact that by selecting only passes giving a high enough density of oxygen to enable oxygen ion temperature to be obtained at the higher altitudes (which correspond to higher latitudes) a premium is put on passes for which the ion temperature is high enough to give an adequate oxygen ion concentration.

REFERENCES

1. M. J. Druyvesteyn. Z. Phys. **64** (1930) 790.
2. G. Medicus. J. Appl. Phys. **33** (1962) 3094.
3. I. Harris and W. Priester. NASA Tech. Note. D–1444 (1962).
4. A. P. Willmore. Proc. Roy. Soc. (In press).
5. A. P. Willmore, R. L. F. Boyd, C. L. Henderson and P. J. Bowen. Proc. Roy. Soc. (1963) (In press).

GEOMAGNETIC CONTROL OF DIFFUSION IN THE UPPER ATMOSPHERE*

S. CHANDRA AND R. A. GOLDBERG

In many recent papers concerned with providing an explanation for the geomagnetic anomaly, agreement with measured data has been obtained from the equations of motion for electrons and ions when used with an empirical boundary condition, whereas poor agreement has resulted from attempts to numerically integrate the commonly employed form of the continuity equation. We have been able to explain this discrepancy by demonstrating that the assumptions used to derive this form of the continuity equations do not agree with observation.

Since the equations of motion do provide a favorable description for the geomagnetic anomaly, we have studied the possible physical models leading to the form of the equations used, and found that although field aligned diffusive equilibrium provides the correct form, a more reasonable assumption concerning electron and ion collisions with neutrals also leads to the same result. We have then been able to provide a more realistic theoretical description of the geomagnetic anomaly by employing an analytic form for the boundary condition which is in better agreement with measurement than those previously used.

Finally, by combining the equations of motion for neutrals, electrons and ions, we have been able to indicate geomagnetic control for the neutral atmosphere in the lower F region of the ionosphere, although the exact shape of this distribution is unknown.

INTRODUCTION

In recent months, it has become increasingly evident that some confusion exists in the understanding of the basic physical mechanisms governing diffusion and the existence of the geomagnetic anomaly in the ionosphere. This apparent confusion arises by comparison of the work of Chandra (1964), (to be referred to as C–1), in which it is shown that the assumption of ambipolar diffusion along a field line cannot lead to geomagnetic control of the charged particles, and such papers as Goldberg and Schmerling (1962, 1963), (to be referred to as GS–I and GS–II), and Goldberg, Kendall, and Schmerling (1964), (to be referred to as GKS), in which this process does appear to produce geomagnetic control of the charged particle density in the ionosphere.

The purpose of this paper is to describe and resolve the confusion which exists in the field at this moment, and then to point out the new problems with which we must contend in order to derive and apply the diffusion equation to ionospheric problems correctly. In addition, a section will be devoted to an improved theoretical description of the geomagnetic anomaly by using an analytic expression for the vertical electron density distribution at the equator which is more in accordance with measurement than the simple Chapman type distribution employed in GKS.

FUNDAMENTAL EQUATIONS AND DEFINITIONS

The major cause of confusion appears to lie in the application of two phrases, viz. *ambipolar diffusion* and *diffusive equilibrium*. Let us investigate and discuss each of these terms to determine how loose usage of them has led to some of the current problems of misunderstanding.

In the normal sense, ambipolar diffusion refers to a plasma in which the negative (electrons) and positive (ions) charges do not move independently due to the influence of the electric field caused by their Coulomb interactions. In this medium, the electrons and ions drift in pairs and this motion of electron-ion pairs is referred to as ambipolar diffusion. The condition for ambipolar diffusion in a neutral plasma is thereby

$$\vec{v}_e = \vec{v}_i = \vec{v} \qquad (1)$$

*Published as *Goddard Space Flight Center Document X-615-64-121*, May 1964.

where $\vec{v}$ is macroscopic velocity and the subscripts e and i refer to electrons and ions respectively. When

$$\vec{v}=0 \tag{2}$$

the condition for diffusive equilibrium is satisfied.

The implications of (1) are quite straightforward, as shown in C–I. In an isothermal atmosphere and in the presence of a magnetic field, this requires $\nabla x(\vec{v}x\vec{B})=0$. In particular, the assumption of field aligned plasma diffusion ($\vec{v}x\vec{B}=0$) can only be satisfied for the trivial case, $\vec{v}=0$, resulting in a hydrostatic distribution of electron density independent of geomagnetic latitude.

On the other hand, favorable comparison between Alouette topside sounder measurements and theoretical calculations of the geomagnetic anomaly has been obtained in GKS by assuming conditions of ambipolar diffusion and diffusive equilibrium along field lines, thereby indicating a possible conflict with the results in C–I. The problem resolves itself once one investigates the meaning of ambipolar diffusion and diffusive equilibrium in the GKS sense.

Let us first write the general equations of motion for neutrals, electrons and ions, respectively, where the subscript n refers to neutral. Following C–I:

$$\frac{n_e m_e m_n}{m_e+m_n}\nu_{en}(\vec{v}_n-\vec{v}_e)+\frac{n_i m_i m_n}{m_i+m_n}\nu_{in}(\vec{v}_n-\vec{v}_i) = -\nabla p_n+n_n m_n\vec{g} \tag{3}$$

$$\frac{n_i m_e m_i}{m_e+m_i}\nu_{ei}(\vec{v}_e-\vec{v}_i)+\frac{n_e m_e m_n}{m_e+m_n}\nu_{en}(\vec{v}_e-\vec{v}_n) = -\nabla p_e+n_e m_e\vec{g}-e\,n_e(\vec{E}+\vec{v}_e\times\vec{B}) \tag{4}$$

$$\frac{n_i m_i m_e}{m_e+m_i}\nu_{ei}(\vec{v}_i-\vec{v}_e)+\frac{n_i m_i m_n}{m_i+m_n}\nu_{in}(\vec{v}_i-\vec{v}_n) = -\nabla p_i+n_i m_i\vec{g}+e\,n_i(\vec{E}+\vec{v}_i\times\vec{B}) \tag{5}$$

where n is number density, ν_{kl} is the collision frequency between the k^{th} and l^{th} particle, m is mass, p is pressure, $\vec{g}$ is gravitational acceleration, e is the absolute value of electron charge, $\vec{E}$ is electric field, and $\vec{B}$ is magnetic field. In writing equations (3)—(5) it is assumed that $\frac{\nu_{lk}}{n_k}=\frac{\nu_{kl}}{n_l}$

In the following we assume that the plasma is in a quasineutral state

$$n_e\approx n_i=N \tag{6}$$

and that the electrons, ions and neutrals obey the ideal gas law in the ionosphere,

$$p_j=n_j kT_j \tag{7}$$

when k is Boltzmann's constant and T is temperature. Furthermore, we assume thermal equilibrium, i.e.

$$T_e=T_i=T \tag{8}$$

Then,

$$p_e=p_i=p \tag{9}$$

In addition, we assume for simplicity that

$$\vec{v}_n\approx 0 \tag{10}$$

Then summation of (4) and (5) provides

$$\frac{m_n m_e N}{m_e+m_n}\nu_{en}\vec{v}_e+\frac{m_n m_i N}{m_i+m_n}\nu_{in}\vec{v}_i=-2\nabla p +N(m_e+m_i)\vec{g}+\vec{J}\times\vec{B} \tag{11}$$

where $\vec{J}$ is current density, defined as

$$\vec{J}=Ne(\vec{v}_i-\vec{v}_e) \tag{12}$$

Since we are investigating ambipolar diffusion and diffusive equilibrium in the GKS sense, it is desirable to write this equation in component form along a field line as

$$\frac{m_n m_e}{m_e+m_n}\nu_{en}\vec{v}_e\cdot\vec{h}+\frac{m_n m_i}{m_i+m_n}\nu_{in}\vec{v}_i\cdot\vec{h} =\left[\frac{-2kT\nabla N}{N}+(m_e+m_i)\vec{g}\right]\cdot\vec{h} \tag{13}$$

where $\vec{h}$ is a unit vector in the direction of the magnetic field. Let us write (13) in more familiar form by using

$$m_e\ll m_i,\ m_n \tag{14}$$

and defining the scale height of the ionizable constituent as H_i, where

$$H_i=\frac{kT}{m_i g} \tag{15}$$

Also, for convenience, we make the approximation

$$m_n\approx m_i \tag{16}$$

Then

$$\frac{m_e\nu_{en}}{2}\vec{v}_e\cdot\vec{h}+\frac{m_i}{4}\nu_{in}\vec{v}_i\cdot\vec{h}=-kT\left(-\frac{\nabla N}{N}+\frac{\vec{i}_r}{2H_i}\right)\cdot\vec{h} \tag{17}$$

Finally, we write

$$\vec{h} = -(\vec{i}_r \sin I + \vec{i}_\theta \cos I) \tag{18}$$

where $\vec{i}_r$ and $\vec{i}_\theta$ are unit vectors in the r and θ directions and I is the magnetic dip angle, reckoned positive when the north seeking pole of the needle points downward. Now, if we treat ambipolar diffusion in the GKS sense, we simply imply that the electron and ion velocity components in the field direction are equal, i.e.

$$\vec{v}_e \cdot \vec{h} = \vec{v}_i \cdot \vec{h} = v_\parallel \tag{19}$$

Applying (18) and (19) in (17), we obtain

$$v_\parallel = \frac{-kT}{\mu\nu}\left[\sin I\left(\frac{1}{N}\frac{\partial N}{\partial r} + \frac{1}{2H_i}\right) + \frac{\cos I}{Nr}\frac{\partial N}{\partial \theta}\right] \tag{20}$$

where

$$\mu\nu = \frac{m_e\nu_{en}}{2} + \frac{m_i\nu_{in}}{4} \tag{21}$$

Assuming that

$$m_e\nu_{en} \ll m_i\nu_{in} \tag{22}$$

because of (14), we may write

$$\mu\nu \approx \frac{m_i\nu_{in}}{4} \tag{23}$$

Equation (20) is a familiar result derived in such papers as Kendall (1962) and GS–II. However, it is clearly not the result of ambipolar diffusion, which is given by (1), but instead, the result of a statement concerning the field line components of electron and ion velocities given by (19).

If we now demand

$$v_\parallel = 0 \tag{24}$$

which is the statement implying diffusive equilibrium along a field line in the GKS sense, we obtain the familiar equation

$$\sin I\left(\frac{1}{N}\frac{\partial N}{\partial r} + \frac{1}{2H_i}\right) + \frac{\cos I}{Nr}\frac{\partial N}{\partial \theta} = 0 \tag{25}$$

which can also be written as

$$\frac{1}{N}\frac{dN}{dr} + \frac{1}{2H_i} = 0 \tag{26}$$

provided we recognize that r and θ are not independent in (25) but related by the dipole field conditions

$$r = r_0 \sin^2\theta \tag{27}$$

and

$$\tan I = 2\cot\theta \tag{28}$$

It is evident that (26) can only be treated in total derivative form if the integration is carried out along the field line.

Statements concerning the components of vectors in a particular direction, such as (19), do not imply any conditions on the total vector. As a result, (25) has not required the assumption of any restrictions on the behavior of the velocity components normal to the field lines.

Equation (26) has been the basis of describing geomagnetic control in the upper F-region in GKS paper. Although (26) has been derived assuming diffusive equilibrium along a field line, it is undesirable to apply this concept because it is of purely hypothetical nature. We now investigate other assumptions to find a more realistic justification for (26).

Let us rewrite (17) as

$$\frac{m_e\nu_{en}}{2}v_{e_\parallel} + \frac{m_i\nu_{in}}{4}v_{i_\parallel} = -kT\left(-\frac{\nabla N}{N} + \frac{\vec{i}_r}{2H_i}\right)\cdot\vec{h} \tag{29}$$

We find two ways for the right hand side of (29) to approach zero. The first imposes a new condition on the velocities, viz:

$$\vec{v}_e = -\frac{m_i\nu_{in}\vec{v}_i}{2m_e\nu_{en}}$$

or

$$v_{e_\parallel} = -\frac{m_i\nu_{in}v_{i_\parallel}}{2m_e\nu_{en}} \tag{30}$$

a result which, although possible, would require a very special condition that the electron velocity be of the order of 10^3 times greater than and in the opposite direction of the ion velocity.

However, if we can demand that the collision frequencies between electrons and neutrals and between ions and neutrals be sufficiently small so that the drag forces arising due to collision be negligible as compared to the pressure gradient, gravity and Lorentz forces it is possible to derive equation (26) without imposing any restriction

on the velocities of electrons and ions. We believe that this assumption is more realistic in the upper F-region where the gyro-frequencies of electrons and ions are much greater than their corresponding collision frequencies.

Although the collision frequency assumption is physically more desirable, it prevents us from obtaining a simple expression for $v_{e\parallel}$ or $v_{i\parallel}$. Instead, we must return to the original equations of motion, (4) and (5), and solve for $\vec{v}_e$ and $\vec{v}_i$ explicitly, as has been carried out in the appendix in C-I. Unfortunately this introduces a very serious complication in the work because of the difficulty in eliminating electric field from the expressions of $\vec{v}_e$ and $\vec{v}_i$ without making specific assumptions about the relationship between $\vec{v}_e$ and $\vec{v}_i$. The implications of these assumptions will be discussed in the latter part of this paper. In the following section we proceed to discuss the physical implications of equation (26).

THE ELECTRON DENSITY DISTRIBUTION WITH A VARIABLE SCALE HEIGHT

Equation (26) can be integrated along a field line to provide the general solution

$$N(r,\theta)=f(r_0,\pi/2)e^{\frac{r\cot^2\theta}{2H_i}} \tag{31}$$

However, if we treat T and m_i constant but recognize that g is proportional to $1/r^2$, H_i is then proportional to r^2, and we obtain

$$N(r,\theta)=f(r_0,\pi/2)e^{\frac{r\cos^2\theta}{2H_i(r)}} \tag{32}$$

In both cases, $f(r_0, \pi/2)$ is an arbitrary function of height at the equator which cannot be determined by the equations of motion from which (31) or (32) are derived. The function $f(r_0, \pi/2)$ must therefore be given as a boundary condition in this problem and can only be determined empirically or by use of additional equations governing the physics of the problem.

Since (31) or (32) depend exclusively upon the equations of motion, it appears that an additional equation, such as the continuity equation, should lead to the desired boundary condition. Unfortunately, as we will show in the next section, the derivation and solution of the continuity equation depend upon a knowledge of $\vec{E}$. Thus, the complexity of the problem becomes quite formidable and it is difficult to anticipate a simple method of solution at this time.

Instead we depend upon an empirical type boundary condition, which may very well be the solution of the correct continuity equation, to derive the explicit form of the electron density distribution.

The incorporation of a Chapman distribution for the boundary condition in (31) leads to the results obtained in CKS. Since such a boundary condition can only be considered as a rough approximation to the shape of the actual vertical electron density distribution at the equator, it is desirable to employ an analytic boundary condition which more closely resembles the true height profiles. Chandra (1963) has proposed a modified form of the Chapman function which includes the effect of variable scale height and which is found to fit the measured vertical distribution for electron density at mid-latitudes far more accurately than the simple Chapman form. We assume here that such a function also describes the vertical electron density distribution at the equator. We can then write

$$f(r_0,\pi/2)=N_{r_{m0}}\exp\frac{1}{2}\left\{1-\frac{r_0-r_{m0}}{H_0\left[1-\alpha\exp\left(-\alpha\frac{(r_0-r_{m0})}{2H_0}\right)\right]}-\exp\left[-\frac{r_0-r_{m0}}{2H_0\left[1-\alpha\exp\left(-\frac{\alpha(r_0-r_{m0})}{2H_0}\right)\right]}\right]\right\} \tag{33}$$

where H_0 is the scale height of the ionic constituent and $N_{r_{m0}}$ is the value of electron density at the equatorial height r_{m0}. The parameter α, which is a measure of departure from the simple Chapman function, and thereby a *shape factor*, is defined as

$$\alpha=\frac{H_0-H(r_{m0})}{H_0} \tag{34}$$

where $H(r_{m0})$ is that value of (Hr_0) at $r_0=r_{m0}$. Also, r_0 is understood to be the radial height specifically at $\theta=\pi/2$.

Although it will not be shown here, (31) and (32) produce nearly identical results in the equatorial region because the small variation of r in the height region of our interest. Furthermore,

the simplified form given by (31) is more convenient for comparison with the results of the GKS paper. We therefore substitute (33) into (31) and obtain

$$N(r,\theta)=N_{r_{m0}}\exp\frac{1}{2}\left\{1-\frac{r\csc^2\theta-r_{m0}}{H_0\left[1-\alpha\exp\left(-\frac{\alpha(r\csc^2\theta-r_{m0})}{2H_0}\right)\right]}+\frac{r\cot^2\theta}{H_t}-\exp\left[-\frac{r\csc^2\theta-r_{m0}}{2H_0\left[1-\alpha\exp\left(-\frac{\alpha(r\csc^2\theta-r_{m0})}{2H_0}\right)\right]}\right]\right\} \tag{35}$$

Equation (35) then provides a general expression for the electron density at all heights and colatitudes provided that we are in a region where the effects of collision can be neglected.

The variation of $N(h,\theta)N_{h_{m0}}$ with colatitude at constant height is shown in Figures 1–4 for various values of α, h_{m0} and H_0. In these figures, we have converted radial height r to altitude h by taking the earth's radius as 6370 km. We have also assumed that $H_0=H_t$ because the effective scale height in (33) approaches H_0 at high altitudes and Chandra (1963) has indicated that H_0 becomes equal to H_t at these altitudes.

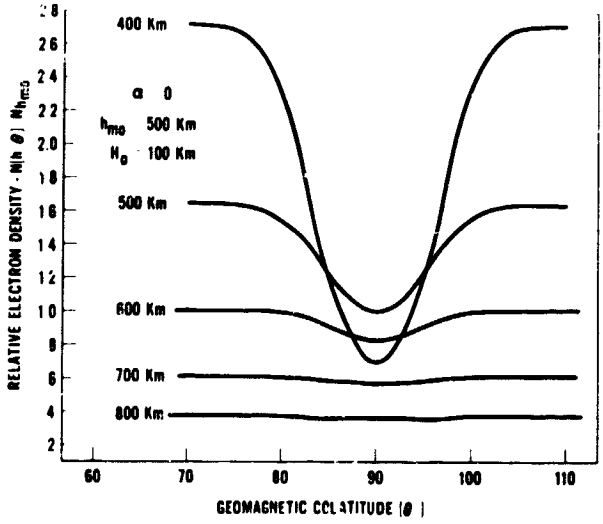

FIGURE 1.—Constant height profiles of relative electron density vs. colatitude for $\alpha=0$, $h_{m0}=500$ km, $H_0=100$ km.

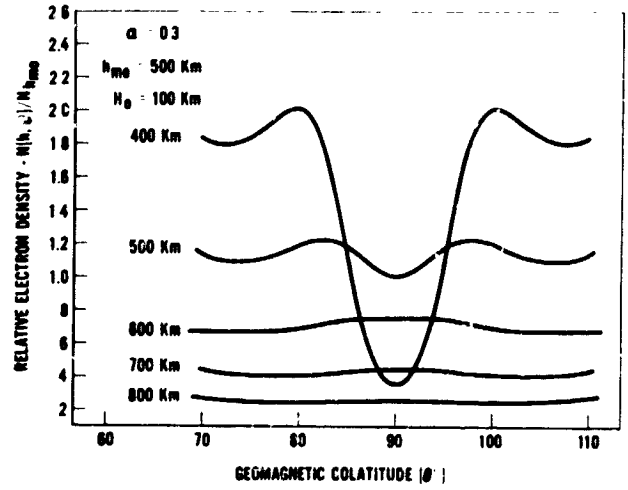

FIGURE 3.—Constant height profiles of relative electron density vs. colatitude for $\alpha=0.3$, $h_{m0}=500$ km, $H_0=100$ km.

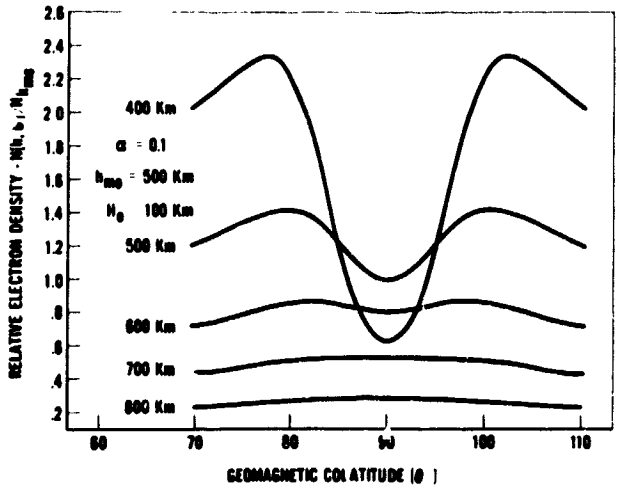

FIGURE 2.—Constant height profiles of relative electron density vs. colatitude for $\alpha=0.1$, $h_{m0}=500$ km, $H_0=100$ km.

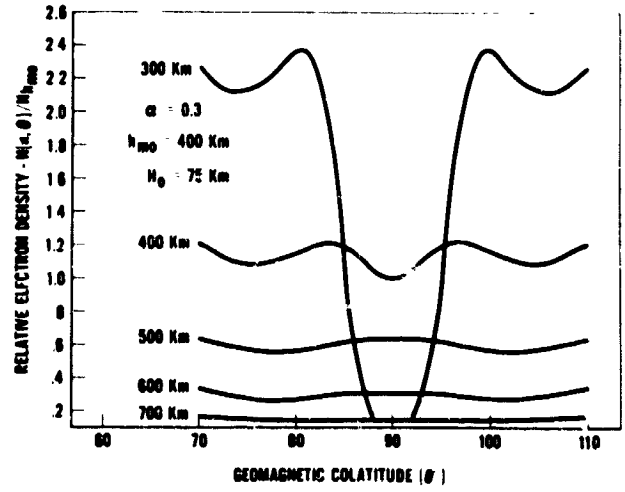

FIGURE 4.—Constant height profiles of relative electron density vs. colatitude for $\alpha=0.3$, $h_{m0}=400$ km, $H_0=75$ km.

We first note that the basic features of the theoretical electron density distribution are unaltered from those first obtained in GKS to describe the geomagnetic anomaly in the vicinity of the equator. Once again the theoretical description breaks down in the bottomside but this is precisely the region where the neglect of momentum transfer terms becomes in-valid. Furthermore, comparison of Figures 3 and 4 clearly shows the insensitivity of the topside results to the parameters h_{m0} and H_0 (except for shifting the constant height profile scale vertically). We therefore conclude the principal properties of the curves can be studied quite extensively by simply altering the shape factor α.

The changes due to variations in α are shown by comparison of Figures 1, 2 and 3. We have also provided a more detailed comparison for one particular height profile in Figure 5. Although

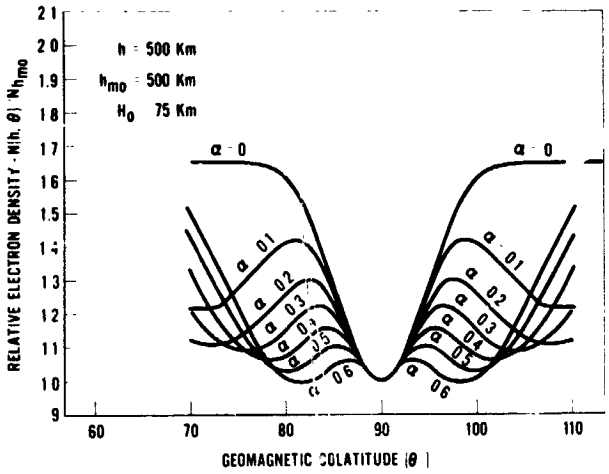

FIGURE 5.—The α dependent behavior of the 500 km profile of relative electron density vs. colatitude for $h_{m0}=500$ km, $H_0=75$ km.

we have included values up to $\alpha=0.6$ to demonstrate the trend of the curves, the highest values are extreme and not likely to be representative of ionospheric conditions. On the other hand, $\alpha=0.1$ to $\alpha=0.4$ are very reasonable values for us to expect under normal conditions representing diurnal and solar cycle variations.

Finally, in equation (35), if we identify the term $H_0[1-\alpha \exp[-\alpha(r \csc^2\theta - r_{m0})/2H_0]]$ with 1/k of the GKS paper, we see that since α is positive, $kH_t>1$ is true for all heights. In particular, if $\alpha=0$, we generate curves which are identical to those in GKS for $kH_t=1$. This explains why $kH_t>1$ provides the closest fit with experimental data in that paper.

PROBLEMS INVOLVED IN THE DERIVATION OF THE DIFFUSION EQUATION

In the previous sections we have seen how the equations of motion for electrons and ions are sufficient to obtain a theoretical description of the electron density distribution in the topside equatorial region of the ionosphere under equinox conditions. This has required us to make certain assumptions concerning collision frequencies or velocity components along field lines and also forced the application of an empirical boundary condition at the equator. In order to produce the empirical boundary condition theoretically and also obtain a solution which is valid in both the topside and bottomside equatorial F region, it is necessary to turn to the continuity equation for additional information. Using the explicit expressions for velocity which are derivable from the equations of motion, it is then possible to derive the diffusion equations associated with the ionosphere.

If we simply require total ambipolar diffusion (equation 1) to occur in the ionosphere so that $\vec{v}$ is independent of the electric field explicitly, and also demand that, in all regions concerned, the motion along field lines are much larger than the drifts normal to field lines, we must then invoke $\vec{v}\times\vec{B}=0$ which, using (4), (5) and (28), gives the constraint equation

$$\frac{1}{N}\frac{\partial N}{\partial r}+\frac{1}{2H}=\frac{2}{N}\frac{\partial N}{r\partial\theta}\cot\theta \qquad (36)$$

This leads to a hydrostatic distribution of electron density which does not agree with measured results, as has been demonstrated in C–I. A second approach (Kendall, 1962, and GS–II) is the assumption that ambipolar diffusion exists only along field lines (see equation (19)). Thus, if we assume that the parallel velocity components of electron and ion velocity are equal and much greater than either of the unequal perpendicular velocity components, we can write (20) as a good approximation for the entire velocity. In mathematical notation, we have

$$\vec{v}\cdot\vec{h}=|\vec{v}_\parallel|=v_\parallel\gg v_{e_\perp},\ v_{i_\perp} \qquad (37)$$

where $v_{e_\perp}$ and $v_{i_\perp}$ are the perpendicular components of electron and ion macroscopic velocities respectively. This implies that

$$\vec{v}_\parallel \approx \vec{v} \tag{38}$$

and provides us with a velocity expression independent of electric field. The general contention has been that (38) allows us to write the steady-state continuity equation in the following form:

$$Q-L=\nabla\cdot N\vec{v}\approx\nabla\cdot N\vec{v}_\parallel \tag{39}$$

where Q and L are production and loss respectively. The procedure has been to substitute (20) into (39) and obtain the well known form of the two dimensional diffusion equation without invoking the equation of constraint (36).

We wish to discuss this approach by first questioning the validity of (37), and then demonstrating that even if it were true, (38) cannot in general imply (39) without the additional inclusion of the constraint equation. This will demonstrate that the field line ambipolar diffusion approach with neglect of the perpendicular velocity components is identical to the total ambipolar diffusion case in which velocities are assumed to lie along field lines. Thus, the results of the two approaches are identical, leading to the conclusion that ambipolar diffusion in which the macroscopic velocity lies along a field line, cannot be the correct physical model to describe the equatorial electron density distribution in the F region of the ionosphere.

Let us first consider (37). We have already seen that the assumption of diffusive equilibrium along a field line ($v_\parallel=0$) leads to a correct description of the electron density in at least the topside region of the ionosphere. If this is the true model of the physical situation, then it is inconsistent with (37) and we cannot expect any results obtained using (37) to provide us with correct results concerning this region. If, on the other hand, the neglect of momentum transfer terms can be attributed to small collision frequencies instead of diffusive equilibrium, (37) need not be violated. This might be a further justification for validating the collision frequency assumption instead of the diffusive equilibrium model. Unfortunately, as we approach the equator, we see from (20) that $v_\parallel$ approaches zero since both sin I and $\partial N/\partial\theta$ approach zero. The latter condition is based strictly upon the empirical condition of symmetry about the equator. We therefore find that no matter how small $v_{e_\perp}$ and $v_{i_\perp}$ may be, there will always be a region about the equator in which (37) does not apply unless

$$v_{e_\perp}=v_{i_\perp}=0 \tag{40}$$

which is identical to the equation of constraint, (36).

We now return to the second question. That is, even if the parallel components of electron and ion velocities are much greater than the perpendicular component, which could still be possible provided $v_{e_\parallel}\neq v_{i_\parallel}$, is it possible to describe the electron density distributions in the entire region of the ionosphere by (39)? We note that

$$\nabla\cdot N\vec{v}=\vec{v}\cdot\nabla N+N\nabla\cdot\vec{v}=(\vec{v}_\parallel+\vec{v}_\perp)\cdot\nabla N+N\nabla\cdot(\vec{v}_\perp+\vec{v}_\parallel) \tag{41}$$

where $\vec{v}$ is now either the electron or ion velocity and

$$\vec{v}=\vec{v}_\parallel+\vec{v}_\perp \tag{42}$$

Now, in order to write (39), we must demand that

$$\vec{v}_\parallel\cdot\nabla N+N\nabla\cdot\vec{v}_\parallel\gg\vec{v}_\perp\cdot\nabla N+N\nabla\cdot\vec{v}_\perp \tag{43}$$

Although (43) could be true for certain special cases, there is not a priori guarantee that (43) will be implied by (37) in general without the additional condition that $v_\perp=0$. Thus, if we are to write (39) as a direct and general implication of (37), we are once again forced to employ the constraint equation.

We cannot state that (40) holds in a very small region about the equator so that its effect outside this region can be neglected. The geomagnetic anomaly itself is a second order effect and we cannot expect to reproduce it by neglecting second order terms which are responsible for its existence.

We therefore find that if ambipolar diffusion exists in the ionosphere, and if it is restricted to the field line direction, we cannot assume (37) without imposing an additional constraint equation. Furthermore, (37) does not generally imply (39) in the ionosphere with or without ambipolar diffusion unless the constraint equation is also employed. However, since (37), (39), and the assumption of ambipolar diffusion along a field line do not provide to the correct description of equatorial electron density, we must conclude that these

assumptions are not valid in a theory leading to a description of the electron density distribution in the equatorial ionosphere.

Kendall (1962), and Rishbeth, Lyon and Peart (1963), have attempted to numerically integrate (39) derived from (20) and (37), without invoking the equation of constraint. They have been unable to obtain the correct description of the geomagnetic anomaly and have therefore concluded that diffusion may not be a very important physical process governing the measured distribution of electron density. However, on the basis of the discussion presented in this section, it now appears that the physical assumptions used in deriving the form of the continuity equation used in their work may not be valid, which simply implies that the diffusion equation is far more complicated than originally believed. Since (19) and (37) are not longer valid, we can no longer equate electron and ion velocities to eliminate electric field. Instead, we must write separate continuity equations for electrons and ions and describe the behavior of electric field before it is possible to obtain the correct theoretical description of the geomagnetic anomaly.

It may appear that the results presented in GS–II are also not valid for the reasons discussed above. However, a closer inspection of GS–II shows that no new information was obtained from the solution of continuity equation than that already available from the equations of motion. The equation discussed in GS–II was simply

$$\nabla\cdot N\vec{v}_{\parallel}=0 \tag{44}$$

where the explicit production and loss terms were neglected in obtaining the series solution. Furthermore, as shown in GKS, the equation of motion leading to (26), whether derived assuming $\vec{v}_{\parallel}=0$, or by making assumptions concerning collision terms, has the identical solution to that obtained from (44) in GS–II. For the case $\vec{v}_{\parallel}=0$, (44) obviously cannot give any new information. This explains why the empirical boundary condition was necessary to obtain a non-arbitrary solution from (44) in GS–II. We should point out, however, that solutions of (39) making use of explicit production and loss terms should not give correct results in the equatorial regions of the ionosphere for the reasons discussed in this section.

THE DISTRIBUTION OF THE NEUTRAL ATMOSPHERE

In this section we will show that when the drag forces are not negligible, as might be the case in the lower F-region and E-region, it is possible to study the behavior of the neutral atmosphere without imposing any restrictions on the velocities of the various constitutents. To obtain the necessary starting equation, we first sum (3), (4) and (5):

$$-\nabla(p_e+p_i+p_n)+(n_nm_n+Nm_i)\vec{g}+\vec{J}\times\vec{B}=0 \tag{45}$$

where we have once again used (14). The component of (45) along the direction of magnetic field is then

$$[-\nabla(p_e+p_i+p_n)+(m_nn_n+m_iN)\vec{g}]\cdot\vec{h}=0 \tag{46}$$

Comparison of (45) and (46) shows that the net force due to pressure gradient and gravity of all particles is perpendicular to the magnetic field and balanced by a current flow force. Next, using (7), (8), (9), (18) and (28), we have

$$\frac{\partial(n_n+2N)}{\partial r}+\frac{\tan\theta}{r}\frac{\partial(n_n+2N)}{\partial\theta}+\frac{n_n}{H_n}+\frac{N}{H_i}=0 \tag{47}$$

where H_n is the scale height of the neutral atmosphere.

Since $N\ll n_n$ and $H_i\approx H_n$, we can write

$$\frac{n}{H_n}+\frac{N}{H_i}\approx\frac{n}{H_n}+\frac{N}{H_n}\approx\frac{n+2N}{H_n} \tag{48}$$

where the suffix on n has been dropped for simplicity. Then (47) becomes, in total derivative form,

$$\frac{d(n+2N)}{dr}+\frac{n+2N}{H_n}=0 \tag{49}$$

Integration of (49) along the field line gives

$$n(r,\theta)\approx n+2N=\vec{g}(r_0,\pi/2)e-\int_{r_0}^{r}\frac{dr}{H_n} \tag{50}$$

where $g(r_0,\pi/2)$ is an arbitrary function of height at the equator and r_0 is defined in (27). If we now demand that the radial distribution of the neutrals obey the normal hydrostatic law at the equator, so that

$$g(r_0,\pi/2)=n_{00}\,e-\int_{r_{00}}^{r_0}\frac{dr}{H_n} \tag{51}$$

where n_{00} is the neutral number density at height r_{00} on the equator, then

$$n(r) = n_{00}\, e - \int_{r_{00}}^{r} \frac{dr}{Hn}, \qquad (52)$$

a result which is entirely independent of θ. If, on the other hand, $g(r_0, \pi/2)$ is perturbed *in any manner* from the exact hydrostatic equilibrium case, we will obtain a distribution for n which does depend on θ. The origin of this angular dependence on the neutrals may seem somewhat surprising until we realize that in selecting a functional form for $g(r_0, \pi/2)$, any deviation in the equatorial neutral distribution from hydrostatic equilibrium must arise due to collisions between neutrals and geomagnetically controlled charged particles. Thus, if the collisions between neutrals and charged particles are sufficiently large to make the momentum transfer forces between charged and neutral particles important, the neutrals will begin to tend toward the angular distribution of the geomagnetically controlled particles. This can also be seen from (3), where it is obvious that we will not obtain the exact hydrostatic distribution in a region when the terms on the left hand side become important. On this basis, we might expect to observe angular variations of the neutral distribution in the bottomside regions of the ionosphere where charged-neutral particle interactions become important.

CONCLUSIONS

From the discussion and results of this paper, we have shown the following:

1. From the equations of motion, it is possible to derive an expression for the electron-density distribution along a field line either by assuming diffusive equilibrium along the direction of the magnetic field or by neglecting the drag forces arising from collisions. The latter assumption appears to be more realistic in the topside of the ionosphere. In either case, it is necessary to assume a radial distribution at the equator to obtain the electron density distribution.

2. We have provided a more accurate formula for the representation of the equinox geomagnetic anomaly than that produced in GKS. Since the empirical boundary condition equation used herein has been shown by Chandra (1963) to fit nearly all vertical profiles of electron density measured to date, we can safely assume that the proper selection of parameters in this formula will lead to a reasonable reproduction of the anomaly in any equatorial region of the ionosphere where interactions of neutrals with charged particles are small because of infrequent collisions.

3. The theory discussed above is semiphenomenological; i.e., it is based on effect and not cause. It does not require a knowledge of the complicated array of physical effects and mechanisms which combine to form the geomagnetic anomaly but, instead, uses an empirical boundary condition which is the accumulated effect of all these causes.

Naturally, if we are to increase our knowledge of the basis mechanisms causing the anomaly and thereby replace the empirical boundary condition by one based on more fundamental considerations than measurement, we must turn to the equations of continuity. Unfortunately, the derivation of the correct continuity equations requires knowledge concerning the electron and ion velocities and/or the electric fields acting on these particles. Currently, most derivations of the continuity equations employ simplifying assumptions, such as $v_{e\parallel} = v_{i\parallel} = v_\parallel$; $v_\parallel \gg v_{e_\perp}, v_{i_\perp}$. The equation derived in the literature under the above assumptions has been numerically integrated by several workers to obtain a theoretical electron density distribution near the equator under steady state conditions. The results obtained by these workers have been unable to account for the gross features of the geomagnetic anomaly, at least to the correct order of magnitude. This has led them to believe that diffusion is of minor importance in governing the geomagnetic anomaly.

We have been able to demonstrate that the velocity assumptions described above do not lead to the proper description of the geomagnetic anomaly. We therefore feel that the assumption about velocities used in the continuity equation rather than the ineffectiveness of motions are responsible for the unsatisfactory description of the geomagnetic anomaly obtained by others.

4. A study of the neutral atmosphere distribution has led us to the conclusion that geomagnetic control of neutrals occurs in any region of the ionosphere where interactions of neutrals with charged particles become important. Since this is most likely to occur in the lower F region of

the ionosphere we suggest that such geomagnetic control of the neutrals might be observable in this region.

ACKNOWLEDGEMENTS

We wish to thank Miss Partica A. Egan for programming the numerical computations used in this work. We also wish to thank Drs. Frank C. Jones and Arnold P. Stokes for many valuable suggestions and critical comments concerning this paper.

Both authors have carried out this research as NAS–NRC Postdoctoral Resident Research Associates.

BIBLIOGRAPHY

CHANDRA, S., *Electron Density Distribution in the Upper F Region*, J. Geophys. Res. **68**, 1937–1942, 1963.

CHANDRA, S., *Plasma Diffusion in the Ionosphere*, J. Atmospheric Terrest. Phys. **26**, 113–122, 1964.

GOLDBERG, R. A. and E. R. SCHMERLING, *The Distribution of Electrons Near the Magnetic Equator*, J. Geophys. Res. **67**, 3813–3815, 1962.

GOLDBERG, R. A. and E. R. SCHMERLING, *The Effect of Diffusion on the Equilibrium Electron Density Distribution in the F Region Near the Magnetic Equator*, J. Geophys. Res. **68**, 1927–1936, 1963.

GOLDBERG, R. A., P. C. KENDALL, and E. R. SCHMERLING, *Geomagnetic Control of the Electron Density in the F Region of the Ionosphere*, J. Geophys. Res. **69**, 417–427, 1964.

KENDALL, P. C., *Geomagnetic Control of Diffusion in the F2 Region of the Ionosphere. I. The Form of the Diffusion Operator*, J. Atmospheric Terrest. Phys. **24**, 805–811, 1962.

KENDALL, P. C., *Geomagnetic Control of Diffusion in the F2 Region of the Ionosphere. II. Numerical Results*, J. Atmospheric Terrest. Phys. **25**, 87–91, 1963.

RISHBETH, H., A. J. LYON and M. PEART, *Diffusion in in the Equatorial F Layer*, J. Geophys. Res. **68**, 2559–2569, 1963.

THE EFFECT OF A VARIABLE ELECTRON TEMPERATURE ON THE EQUATORIAL ELECTRON DENSITY DISTRIBUTION IN THE UPPER IONOSPHERE

RICHARD A. GOLDBERG

By incorporating a model for the measured electron temperature distribution at the magnetic equator in the isothermal and temperature equilibrium theory of Goldberg, Kendall and Schmerling [J. Geophys. Res., *69*, 417–427, 1964], it has been possible to gain further insight into the behavior of the equatorial geomagnetic anomaly under steady state and equinoctial conditions. In particular, it is shown that the measured deviation from thermal equilibrium in the bottomside ionosphere is very influential in allowing extension of the previous theoretical description of the geomagnetic anomaly well into the bottomside ionosphere and to higher latitudes than originally applicable. For completeness, the effect of gravitational variation is now included, but it is shown that this alone contributes only minor improvements to the original results. Finally, several less common properties in the behavior of the geomagnetic anomaly are investigated, and it is shown under what conditions these secondary effects will occur.

INTRODUCTION

The theory describing the equatorial electron density distribution under conditions of thermal equilibrium, equinox, and steady state, originally presented in Goldberg and Schmerling [1963, 1964] and improved upon in Goldberg, Kendall and Schmerling [1964] (to be referred to as GKS), has provided reasonably good agreement when comparison is made to the measured results of the Alouette Topside Sounder Satellite. Furthermore, Chandra and Goldberg [1964] (to be referred to as CG) have demonstrated that the rather artificial concept of field line diffusive equilibrium need not be employed to obtain the necessary equations, but instead, the neglect of collisions between charged and neutral particles is sufficient in this aim. This has enabled us to understand why the theoretical results agree best with data in the topside ionosphere, since this is the region where such an assumption is most reasonable.

Recent theoretical considerations (Hanson and Johnson, 1961; Hanson, 1962; Dalgarno et al, 1963) and recent measurements with rocket probes (Spencer et al, 1962; Brace et al, 1963) and radar backscatter techniques (Evans, 1962 and 1964; Bowles, 1964) have now demonstrated that thermal equilibrium (electron temperature T_e = ion temperature T_i) does not occur in the lower F region ionosphere during the day including that time when the electron density is experiencing nearly steady conditions. It is the purpose of this paper to provide a simple analytical approach for including a temperature model, based on the theoretical or measured T_e distribution, in the theory discussed in GKS and CG and to demonstrate the possible effects of deviation from conditions of thermal equilibrium on the topside electron density distribution. Furthermore, it will be shown how inclusion of this T_e distribution has allowed extension of the theory into part of the bottomside F layer. Comparison with data is also made to provide a possible explanation of several features of the geomagnetic anomaly heretofore unexplained. For completeness, the effects of variable gravity are also included and the slight modifications in the results due to this effect are demonstrated.

*Published as *Goddard Space Flight Center Document X-615-64-279*, October 1964.

SYMBOLS

$\vec{B}$	magnetic field of earth
e	absolute value of electron charge
$\vec{g}$	gravity
H_e	electron density scale height
H_i	ionizable constituent scale height; cf. (16)
H_p	value of H_i at r_p
H_T	scale factor of temperature
H_τ	cf. (7)
$\vec{h}$	unit vector in direction of $\vec{B}$
h_mF2	height of $F2$ layer electron density peak
I	magnetic dip angle; cf. (10)
$\vec{i}_r$, $\vec{i}_\theta$	polar coordinate unit vectors
$\vec{J}$	current density; cf. (3)
K	value of T_e/T_i at r_p
k	Boltzmann's constant
m	mass
N, n	number density; cf. (2)
N_{m0}	equatorial peak electron density
N_mF2	$F2$ layer peak electron density
p	pressure
R	mean radius of earth (6370 km)
r	radial height ($r=z+R$)
r_{m0}	height of equatorial peak electron density
r_0	equatorial radial height
r_p	radial height of temperature peak
T	temperature
$\vec{v}$	velocity
z	altitude
θ	colatitude
ν_{jk}	collision frequency between j^{th} and k^{th} particles
τ	average of electron and ion temperatures; cf. (6)

SUBSCRIPTS

e, i, n	electrons, ions, and neutral particles respectively
m	peak value
mo	equatorial peak value

THE FUNDAMENTAL EQUATION

From CG, combination of the equations of motion for electrons and ions provides

$$Nm_e\nu_{en}\vec{v}_e+\frac{Nm_im_n}{m_i+m_n}\nu_{in}\vec{v}_i= -\nabla p_e-\nabla p_i+Nm_i\vec{g}+ir\,\vec{J}X\vec{B} \quad (1)$$

where we have assumed

$$\begin{aligned} v_n &\ll v_e,\ v_i \\ m_e &\ll m_i,\ m_n \\ n_e &= n_i = N \end{aligned} \quad (2)$$

In (1) and (2), the subscripts e, i, and n refer to electrons, ions, and neutrals respectively; p is pressure; n is number density; ν_{jk} is collision frequency between the j^{th} and k^{th} particles; m is mass; v is velocity; g is gravitational acceleration; B is the earth's magnetic field; and J is current density defined as

$$\vec{J}=Ne(\vec{v}_i-\vec{v}_e) \quad (3)$$

where e is the absolute value of electron charge.

If now, we assume that ν_{en} and ν_{in} are sufficiently small to allow neglect of the drag forces, then

$$-\nabla p_e-\nabla p_i+N\,m_i\vec{g}+\vec{J}X\vec{B}=0 \quad (4)$$

Assuming the electrons and ions behave as ideal gases and taking the field line component of (4), we obtain

$$[-Nk\nabla(T_e+T_i)-(T_e+T_i)k\nabla N+Nm_i\vec{g}]\cdot\vec{h}=0 \quad (5)$$

where T_j is the temperature of the j^{th} type particle, k is Boltzmann's constant, and $\vec{h}$ is a unit vector in the direction of the earth's magnetic field.

Let us define

$$\tau=\frac{T_e+T_i}{2} \quad (6)$$

$$H_\tau=\frac{k\tau}{m_ig} \quad (7)$$

Then

$$\left(\frac{\nabla\tau}{\tau}+\frac{\nabla N}{N}+\frac{\vec{i}_r}{2H_\tau}\right)\cdot\vec{h}=0 \quad (8)$$

where $\vec{i}_r$ is a unit vector in the radial direction. If we assume that the earth's magnetic field is a dipole lying in the r, θ plane, we obtain

$$\frac{1}{\tau}\left(\frac{\partial\tau}{\partial r}\sin I+\frac{1}{r}\frac{\partial\tau}{\partial\theta}\cos I\right)+\frac{1}{N}\left(\frac{\partial N}{\partial r}\sin I+\frac{1}{r}\frac{\partial N}{\partial\theta}\cos I\right)+\frac{\sin I}{2H_\tau}=0 \quad (9)$$

where I is the magnetic dip angle defined by

$$\tan I = 2\cot\theta \tag{10}$$

and θ is geomagnetic colatitude. (In the following discussion, all coordinates given are geomagnetic.) As pointed out in CG, (9) can be written in total derivative form as

$$\frac{d\tau}{\tau}+\frac{dN}{N}+\frac{dr}{2H_\tau}=0 \tag{11}$$

provided the integration is carried out along a field line. The solution of (11) is

$$N(r,\theta)=N(r_0)\frac{\tau(r_0)}{\tau(r,\theta)}e^{-\int_{r_0}^{r}\frac{dr}{2H_\tau}}$$

where r_0 is the equatorial height of the field line of integration, i.e.

$$r_0 = r\csc^2\theta \tag{13}$$

and $N(r_0)$, $\tau(r_0)$ represent the vertical distributions of N and τ at the equator.

THE BOUNDARY CONDITIONS

From (12), it is clear that the complete temperature distribution, given by $\tau(r,\theta)$, must be known in addition to the radial distribution of N at the equator, $N(r_0)$, before $N(r,\theta)$ can be determined uniquely. In previous work, $\tau(r,\theta)$ has simply been specified as a constant everywhere. We now investigate the properties of the theoretical electron density distribution when we include a simple radial model for τ based on measurement and theory.

Recent rocket probe measurements (Spencer, et al, 1962 and Brace, et al, 1963) at Wallops Island, Virginia, show a vertical electron temperature profile under quiet day conditions which departs from the ion temperature at 150 km, peaks between 200 and 250 km with a value of $T_e \approx 2T_i$, and then returns to the $T_i = T_e$ value at about 350 km. Evans [1962] obtains a similar type behavior and later [1964] shows improved results which indicate a peak at 300 km and a return to $T_e/T_i = 1$ above 700 km for radar backscatter measurements in the midlatitude region of Boston, Mass. The only measurements available in the equatorial region are those of Bowles [1964] using the backscatter technique and he reports a T_e/T_i peak value of 2 occurring at about 275 km. Furthermore, he never finds $T_e/T_i > 1$ above 400 km.

Hanson and Johnson [1961], Hanson [1962] and Dalgarno et al [1963] have presented theoretical models for T_e/T_i based on local EUV heating which result in similar type profiles to those measured, viz. $T_e/T_i = 2$ at the peak with the peak occurring between 200 and 250 km. The theoretical models are probably most representative of the equatorial regions where EUV heating is most likely to predominate. The theoretical peak height is somewhat lower than that reported by Bowles [1964] but Dalgarno et al [1963] explain that their lower value for the peak can be attributed to an underestimate of the cooling rate by neglect of the contribution from vibrational excitations. They also state that one should expect a more rapid cooling rate in a warmer atmosphere and this appears to indicate a higher altitude for the T_e/T_i peak at times of higher sunspot number. These are important considerations in selecting the numerical values for the height of the electron temperature peak (r_p) in the next section.

The results discussed above clearly demonstrate the absence of thermal equilibrium in the lower F region of the ionosphere. Unfortunately, the data and theoretical models available are rather limited and the exact behavior and distributional shape is currently rather uncertain. As a reasonable first guess, we therefore choose a simple analytic distribution for T_e which is representative of any of the above profiles but which does not fit any of them in an exact sense. We also consider the temperature behavior to be independent of latitude in the equatorial region under consideration (i.e. from 20°N to 20°S).

An expression which possesses these qualifications is

$$T_e = T_i\left[1+\frac{K-1}{1+\frac{(r-r_p)^2}{H_T^2}}\right] \tag{14}$$

where K is the ratio T_e/T_i at the peak height (r_p) of the T_e distribution and H_T is a scaling factor which governs the thickness of the T_e distribution and which will be referred to as the thermal scale height. A typical plot of (14) is shown in Figure

1 for various values of H_T and for $r_p = 6650$ km. From (14), we obtain

$$\tau(r, \theta) = \tau(r) = \frac{T_i}{2}\left[2 + \frac{K-1}{1+\frac{(r-r_p)^2}{H_T^2}}\right] \quad (15)$$

Although the effect of the gravitational height dependence is small, we include it for completeness in the work which follows. The scale height of the ionizable constituent is given by

$$H_i = \frac{kT_i}{m_i g} \quad (16)$$

If we define H_p as that value of H_i at the height r_p, i.e. the matching point, and we treat T_i as constant in the region under consideration, then

$$H_i = \frac{r^2}{r_p^2} H_p \quad (17)$$

With these definitions, we have

$$H_\tau = \frac{H_p}{2}\frac{r^2}{r_p^2}\left[2 + \frac{K-1}{1+\frac{(r-r_p)^2}{H_T^2}}\right] \quad (18)$$

The form of H_τ given by (18) allows explicit integration of the integral in (12). We obtain

$$-\int_{r_0}^{r} \frac{dr}{2H_\tau} = \frac{r_p^2[F_1+F_2+F_3+F_4]}{2H_p\left[r_p^2 + \frac{H_T^2(K+1)}{2}\right]^2} \quad (19a)$$

where

$$F_1 = \left[r_p^2 - H_T^2\frac{(K+1)}{2}\right]\left[\frac{H_T(K-1)}{2\left(\frac{K+1}{2}\right)^{\frac{1}{2}}}\right]\left[\tan^{-1}\left(\frac{r-r_p}{H_T\left(\frac{K+1}{2}\right)^{\frac{1}{2}}}\right) - \tan^{-1}\left(\frac{r_0-r_p}{H_T\left(\frac{K+1}{2}\right)^{\frac{1}{2}}}\right)\right] \quad (19b)$$

$$F_2 = r_p H_T^2\left(\frac{K-1}{2}\right)\ln\left[\frac{(r_0-r_p)^2 + H_T^2\left(\frac{K+1}{2}\right)}{(r-r_p)^2 + H_T^2\left(\frac{K+1}{2}\right)}\right] \quad (19c)$$

$$F_3 = 2r_p\left[\frac{K-1}{2}H_T^2 \ln r/r_0\right] \quad (19d)$$

and

$$F_4 = \frac{r_0 - r}{r\, r_0}\left[\left(r_p^2 + \frac{H_T^2(K+1)}{2}\right)(H_T^2 + r_p^2)\right] \quad (19e)$$

Finally, we must apply an analytic form for $N(r_0)$. Although Chandra (1962) formulated an improved functional form for $N(r)$ than that described by the simple Chapman function and this has been incorporated in the results of CG, it is necessary to return to the simple Chapman function in the work that follows in order to make direct comparison with Goldberg, Kendall and Schmerling (1964). Hence, we let

$$N(r_0) = N(r_{m0})e^{\frac{1}{2}\left[1 - \frac{r_0 - r_{m0}}{H_e} - e^{-\frac{r_0 - r_{m0}}{H_e}}\right]} \quad (20)$$

where H_e is the electron density scale height at the equator and N_{m0} is the value of electron density at the vertical peak height r_{m0}.

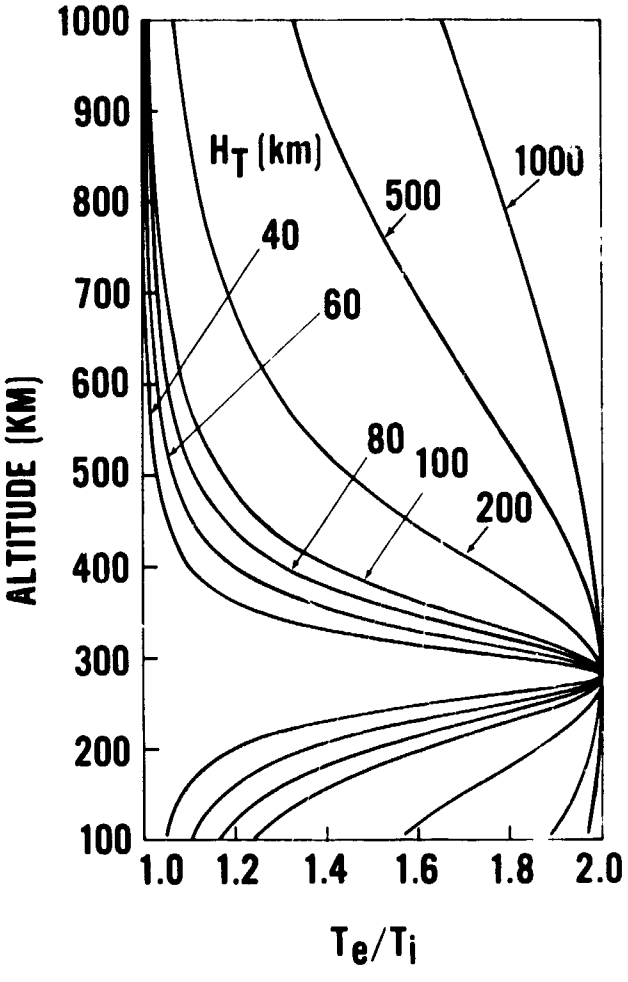

FIGURE 1.—The vertical electron temperature model.

NUMERICAL ANALYSIS AND DISCUSSION

A. The Effect of Gravity

The expressions given by (15), (19) and (20) have been incorporated in (12) to provide an analytic expression for the electron density near the geomagnetic equator above and below the electron density peak under conditions of steady state and equinox. This expression has then been programmed on an IBM 7094 to allow extensive study of its behavior under wide variations in the temperature parameters. The discussion which follows demonstrates how adjustment of the parameters governing the temperature distribution leads to variations in the properties of the geomagnetic anomaly.

Before investigating the actual effect of a variable T_e, let us first study the change induced by simply adding the gravity variation. This is obtained by replacing H_r with H_i and treating $\tau(r,\theta)$ as a constant in (12). Then

$$N(r,\theta)=N(r_0)e^{\frac{r\cos^2\theta}{2H_i}} \tag{21}$$

where H_i possesses the functional dependence on height given by (17). This can be compared to the constant H_i result employed in GKS, viz.

$$N(r,\theta)=N(r_0)e^{\frac{r\cot^2\theta}{2H_p}} \tag{22}$$

where H_2 of GKS is now H_p. (In the discussion and results which follow, the scale height of the electron density distribution H_e has also replaced $1/k$ in GKS notation).

Comparison of (21) and (22) shows that very little change in results should be expected in that region of latitude where $\cot\theta$ and $\cos\theta$ are comparable in magnitude. This encompasses nearly the entire region of our interest. This conclusion is borne out by numerical comparison of (21) and (22) for cases in which $H_p/H_e>1$. A more important result is obtained for cases presented in GKS for $H_p/H_e\leq 1$. In that paper it was shown that angular peaks could not be obtained for this range of selection in parameters, although the initial rise with latitude behaved in equivalent manner to the geomagnetic anomaly. The simple inclusion of gravity now rectifies this situation by allowing angular peaks to form for these cases.

A comparison of the 380 km and 480 km electron density profiles with and without gravity variation for $H_p/H_e=1$ is shown in Figure 2 using the numerical parameters given in Table 1 (The altitude z is related to radial distance r by $r=z+6370$ km). Curve a represents the constant g case given by (22). Curves b and c represent variable $g(r)$ cases in which the matching of H_i with H_p is taken to be at two different heights, viz. 6650 and 6850 km, respectively. We first note that the effect of varying the matching point is rather small and has little if any influence on the features we wish to discuss. We also find that regardless of matching point height, the curves stay relatively close even at high latitudes. The generation of an angular peak for $r_p=6650$ km is not surprising since $H_i/H_p>1$ everywhere above r_p. However, it is surprising to find this result for the 380 km (6750 km) profile when $r_p=6850$, since $H_i/H_e<1$ at this height. This result occurs for all cases investigated and we must conclude that although gravity is a small effect in altering the slope of the curves, as comparison of curves 2b and 2c demonstrate, it is a strong effect in providing a more realistic description of the geomagnetic anomaly should it occur under conditions where $H_p/H_e\leq 1$.

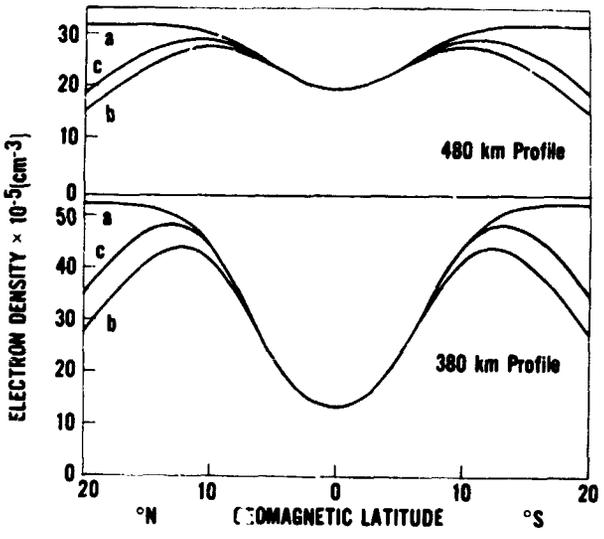

FIGURE 2.—The influence of the gravity variation on a horizontal electron density profile for $H_p/H_e=1$; a) constant g, b) and c) variable g.

B. The Effect of Temperature

Although inclusion of height dependent gravity, $g(r)$, appears to resolve the problem of theoretically describing the geomagnetic anomaly

when $H_i/H_e \leq 1$, it has been shown in CG that this condition is a rather unlikely situation to occur on both empirical and physical grounds. We therefore restrict ourselves in the discussion which follows to $H_i/H_e > 1$.

There are seven parameters to be varied in this problem on the basis of empirical conditions, viz. N_{m0}, r_{m0}, H_e, H_p, H_T, r_p and K. In GKS, it was shown that variation of the first four parameters leads to a description of the equinoctial noontime geomagnetic anomaly during various phases of the solar cycle. Furthermore, although differences in the magnitude and height range of the anomaly occur between high and low sunspot number, no changes in the basic features ascribed to this effect are expected. We will, therefore, limit ourselves to an analysis of the high sunspot case with the knowledge that the results obtained are similar but less pronounced for the intermediate and low sunspot cases. The choice of values for the first four parameters listed above have been made to coincide with GKS by selecting

$$N_{m0} = 19.25 \times 10^5 \text{ electrons/cm}^3,$$

$$H_e = 100 \text{ km}, \; r_{m0} = 6850 \text{ km},$$

and $$H_p = 112.5 \text{ km}.$$

Selection of H_p at the given value insures $H_i/H_e > 1$ in the entire region of interest. The values of the other numerical parameters used are given in Table 1. (These values are selected to coincide as accurately as possible with the temperature profile discussed earlier).

TABLE 1.

Figure	Curve	r_p (km)	H_T (km)	K
1	----------	6650	Variable	2
2	a	----------	0	1
	b	6650	0	1
	c	6850	0	1
3	----------	6650	40	2
4	----------	6650	40	2
5	----------	6650	40	2
6A	----------	Variable	40	2
6B	----------	6850	40	Variable
6C	----------	6850	Variable	2
8	----------	6850	40	2
9	----------	6850	40	2
10	----------	6775	40	2

We can therefore reduce the problem to a three parameter study; H_T and K which determine the thickness and magnitude of the T_e peak respectively; and r_p, which determines the relative distance between the electron temperature and density maxima.

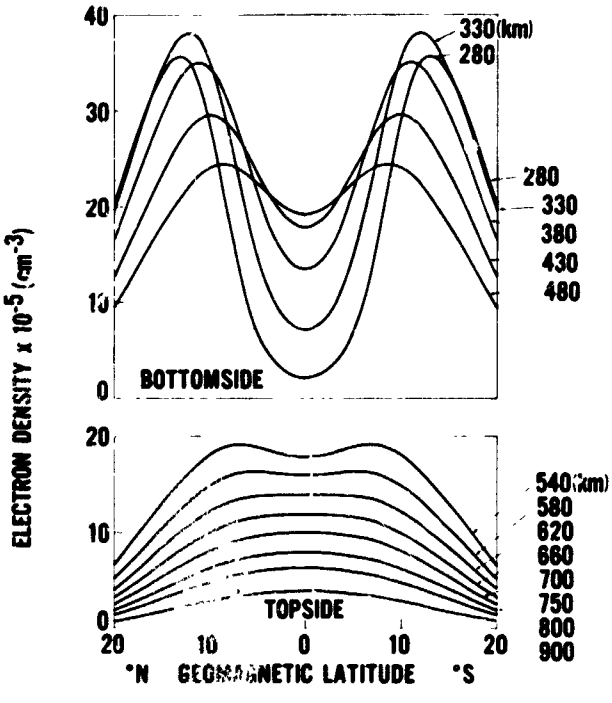

FIGURE 3.—Horizontal profiles of electron density under conditions of variable electron temperature.

Figure 3 represents a sequence of electron density constant height profiles under the effects of T_e variation. Figure 4 represents an equivalent set of vertical profiles. The temperature profile used is illustrated in Figure 1 with parametric values selected for reasons discussed in a previous section.

Comparison of Figure 3 to the thermal equilibrium, constant gravity results given in GKS shows very little modification of the curves out to the angular peak. On the high latitude side of the peak, however, we find a more rapid decrease of electron density in better agreement with measured profiles. This effect is due primarily to the inclusion of the gravitational variation and not the variation in T_e.

A more important result, and one which is entirely due to a variable T_e, is evident in Figure

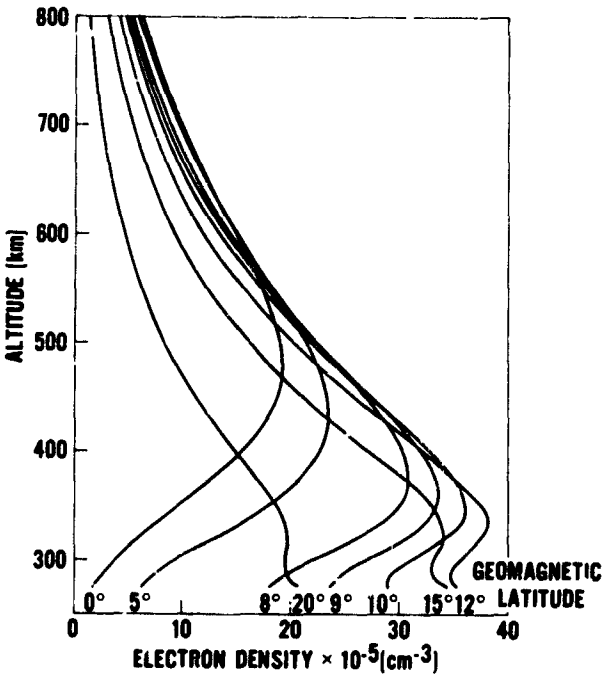

FIGURE 4.—Vertical profiles of electron density under conditions of variable electron temperature.

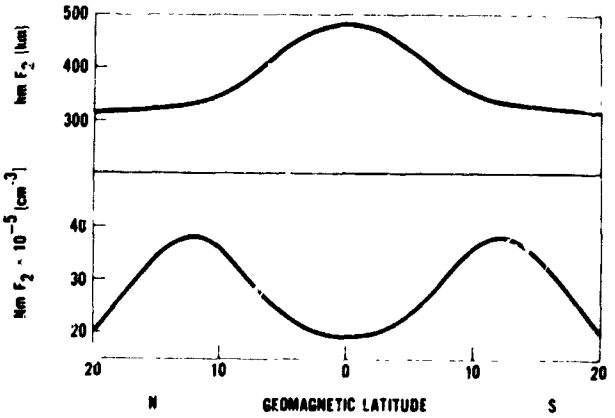

FIGURE 5.—Behavior of N_mF2 and h_mF2 with latitude under conditions of variable electron temperature.

4. We now find qualitative results which match measured data to a height nearly two electron scale heights (H_e) below the equatorial $F2$ peak before discrepancies begin to occur. Since the vertical profiles show a departure from measurement below this height, it appears that the neglect of friction terms in the equations of motion is no longer valid below this region. Nevertheless, it is a valuable extension of the theory to find that the effect of collisions can be neglected to heights well below the equatorial $F2$ peak, especially since it appeared by the results of GKS that collisions were important everywhere below this peak, i.e. in GKS results obtained below the peak do not agree with data and the vertical peaks shown in Figure 4 of this work could not be produced.

The variation of the peak electron density N_mF2 with latitude is given in Figure 5. We observe that a variable T_e produces angular peaks in N_mF2 in accord with measurement, (cf. Croom et al, 1959) whereas in GKS, it was shown that thermal equilibrium is incapable of producing the angular "turnover." Furthermore, this result must be attributed to a variable T_e, since inclusion of variable gravity alone does not alter the results for this parameter given in GKS. The variation of the height of the $F2$ peak, h_mF2, is also given in Figure 5. We observe a leveling out of this height at higher latitudes in accord with measurement (cf. Thomas, 1962), a result which also is not available under thermal equilibrium considerations. A study of these quantities show that their magnitude and shape are very stable to wide variations in K, H_T and $r_{m0}-r_p$, except when K and H_T become very small, i.e. $H_T \leq 29$, $K \leq 1.2$. At these and smaller values we find a rapid transition into the forms published in GKS for thermal equilibrium, in which h_mF2 drops steadily with latitude and N_mF2 rises with latitude without showing any angular peaks.

Figure 6A demonstrates the variation of a typical constant height profile with r_{m0}, viz. 380 km, holding K and H_T fixed. We note that as r_p approaches r_{m0}, the original angular peak converts into a sharper peak adjacent to a relatively flat "ledge." Further study has shown that this effect is not dependent on the absolute value of r_{m0} or the relative distance between the actual constant height profile and r_{m0}. Instead, this behavior is exclusively dependent on $r_{m0}-r_p$.

Because the results which follow depend only on the relative separation $r_{m0}-r_p$ and not on the absolute values of r_p and r_{m0}, and because of the discussion in an earlier section explaining how r_p can actually be larger in a warmer (high sunspot number) ionosphere, we have selected the relatively high value of $r_p \approx r_{m0} = 6850$ km. If the condition $r_p = r_{m0}$ occurs at a lower height, the same results will occur simply shifted this distance in altitude. From Figure 6A we find that the new effect is not present until r_p is very nearly

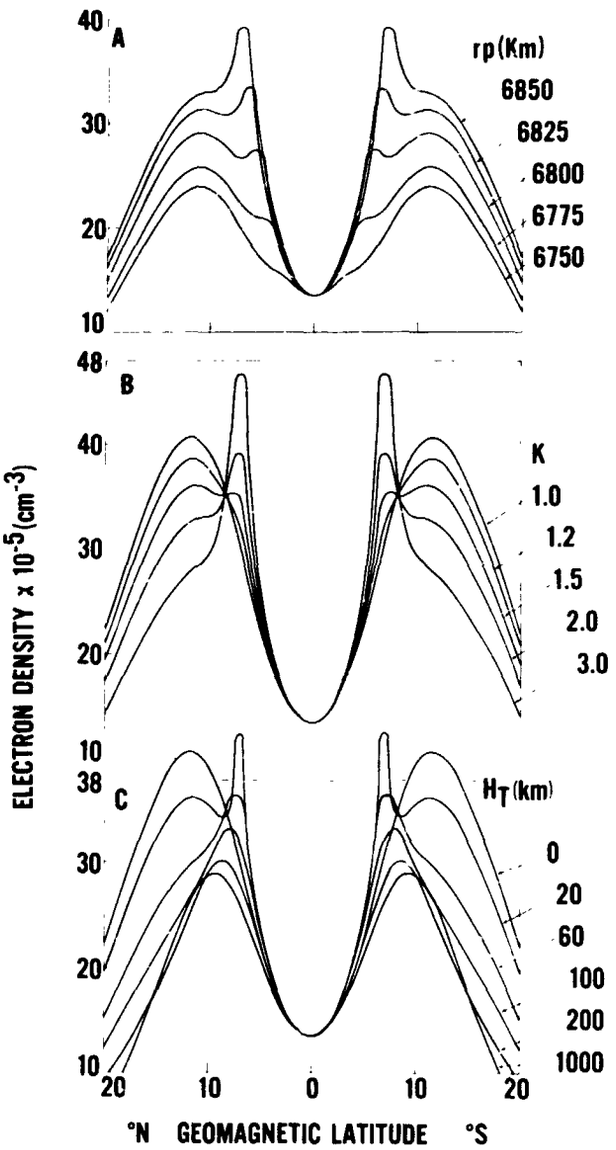

FIGURE 6.—Behavior of a constant height electron density profile (6750 km) with *A*) relative distance between electron temperature and density peaks, *B*) magnitude of temperature peak, *C*) thickness of temperature peak.

equal to r_{m0}, and becomes more pronounced as r_p increases (or r_{m0} decreases).

Although the above effect is not always present, it has appeared in measurements of King et al (1963), an example of which is shown in Figure 7. No attempt has been made to accurately fit this particular profile, however, since there are many combinations of the seven parameters available for such a fit and the profiles showing this property best in the published literature do not always represent noon equinox conditions. Nev-

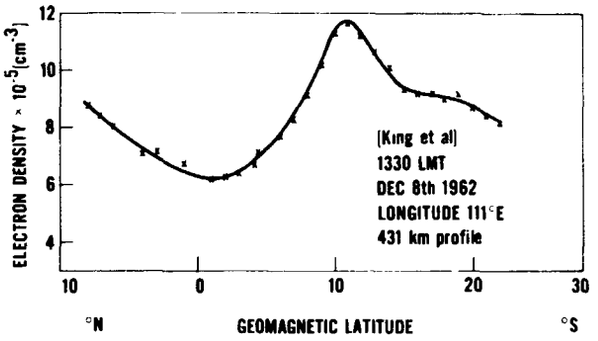

FIGURE 7.—The 431 km electron density profile (King et al, 1963) for December 8, 1962, 1330 LMT, using ALOUETTE data.

ertheless, the effect does occur, and this indicates that the electron temperature and density peaks do lie relatively close together at certain times. During such an occurrence, we would expect the geomagnetic anomaly to appear in a form similar to the result given in Figure 8, where we notice a

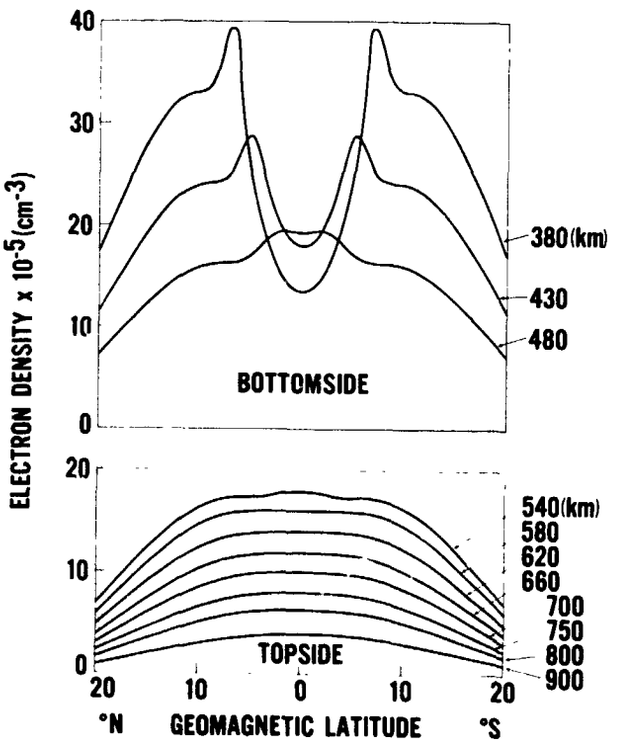

FIGURE 8.—Horizontal profiles of electron density under conditions of variable electron temperature for $r_p = r_{m0}$.

low latitude "ledge" replacing the low latitude "trough" at higher altitudes. We also note a reduction in the height above which the anomaly disappears.

The sequence of vertical profiles corresponding to Figure 8 ($r_p = r_{m0}$) are shown in Figure 9. We

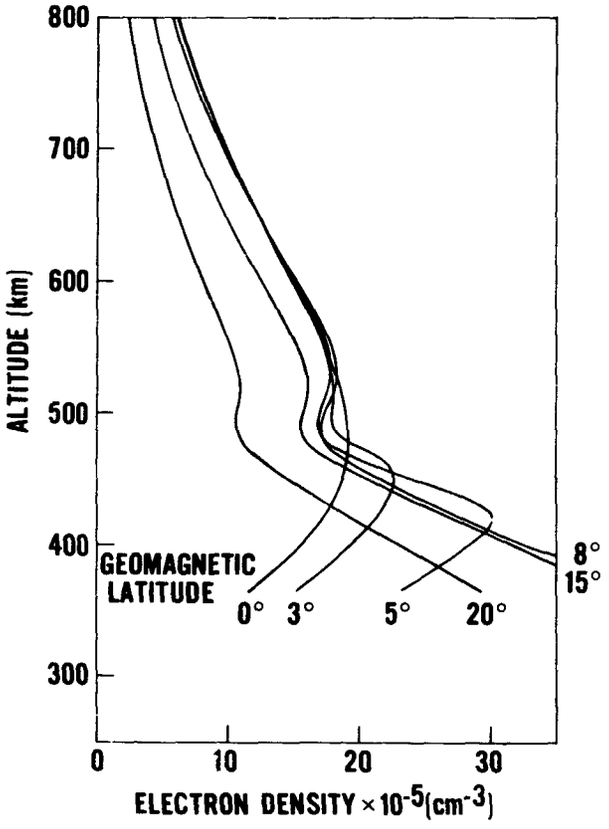

FIGURE 9.—Vertical profiles of electron density under conditions of variable electron temperature for $r_p = r_{m0}$.

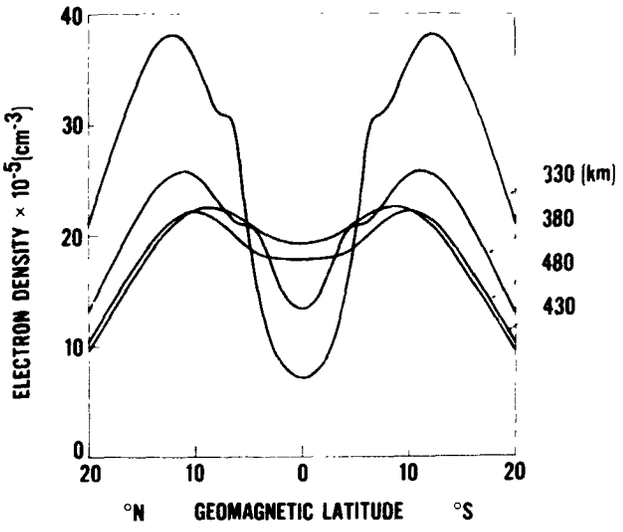

FIGURE 10.—Horizontal profiles of electron density showing the "inner ledge" effect.

find that this extreme lowering of the electron density peak (or raising of the temperature peak) leads to an additional small "bump" in the topside region.

Other smaller effects are also seen upon more detailed study of the results. For example, if $r_{m0} - r_p$ is of the order $.75H_e$ (see Figure 6A), we find the sequence of horizontal profiles illustrated in Figure 10, demonstrating a much smaller ledge occurring on the low latitude side of the angular peaks with no ledge present on the high latitude side. The topside results in this case are identical to those of Figure 3. The determination of this behavior from measurement is difficult, however, because of the small magnitude of the effect.

As partially shown in Figures 6B and 6C, a study of the variations of both K (temperature peak magnitude) and H_T (temperature peak thickness) do not lead to any new conclusions but form a consistent picture, i.e. as K decreases, the ledge gradually disappears leaving the normal horizontal profile for the variable gravity case. As H_T decreases, the effect first sharpens before disappearing for $H_T \leq 15$ km. Similarly, as K and H_T decrease, the topside "bump" in the vertical profile (cf. Figure 9) gradually lowers and blends with the single peak obtained under variable gravity conditions alone. Increasing H_T and K improves the results on the bottomside by reducing the magnitude of the electron density profiles to more reasonable values in this region. Increasing H_T also sharpens the angular peak slightly. Finally, if we consider cases of very large H_T, such as $H_T = 1000$ km, we find a behavior very similar to the $H_T = 0$ situation. This demonstrates that it is the gradient of T_e/T_i, and not its magnitude, which is mostly responsible for the results involving the effect illustrated in Figure 7.

SUMMARY AND CONCLUSIONS

The theory presented in GKS has been extended to include the effects of the variation in gravity and an electron temperature profile based upon empirical and theoretical results. This extension in the theory has led to distinct improvements in the theoretical description of the geomagnetic anomaly when comparison with data is made.

The inclusion of gravitational variation alone has led to an increased gradient on the high latitude side of the theoretical constant height profiles representing the geomagnetic anomaly, this being in better accord with measurement. Furthermore, for the cases in which $H_i/H_e \leq 1$, we now

find angular peaks occurring in the constant height profiles, something which was not available under constant gravity considerations.

The inclusion of an electron temperature vertical profile creates results which are far more remarkable, however. We now obtain a description of the geomagnetic anomaly to heights as low as $2H_e$ below the F2 peak at the equator, thereby indicating that the neglect of friction or collision terms in the equation of motion is allowable down to these heights. The theoretical behavior of N_mF2 and h_mF2 are also found to agree with measurement out to midlatitudes and an angular peaking of N_mF2 is seen to occur. These are results which could not be obtained in GKS under isothermal conditions and thermal equilibrium.

Although T_i has been treated as a constant in the derivation of the expression used to obtain these results, this is not considered to be a serious limitation in the theory since the major gradients in T_i currently appear to be considerably smaller than those in T_e and occur in the very lowest sector of the region under consideration.

Further study with a variable T_e shows that as the height of the electron temperature and density peaks approach one another, we can expect to find an interesting change in the shape of the horizontal electron profiles describing the geomagnetic anomaly. Experimental evidence is presented to show that this behavior does occur at certain times. We also find that the slope of the electron temperature peak rather than its magnitude is more responsible for this effect. In addition, the vertical profiles undergo a slight modification with the appearance of a small "bump" in the topside above h_mF2 during its occurrence. It should be noted, however, that the evidence given in Figure 7 is a topside result and the theoretical results of Figure 8 do not show this effect extending into the topside. Assuming that 431 km was slightly above r_{m0} in Figure 7, we must conclude that either r_p was slightly higher than r_{m0} or that $r_p = r_{m0}$ with the temperature peak exhibiting a sharp gradient (large K, small H_T) on that day, since these are the only possible methods for theoretically obtaining this effect in the topside with the temperature profile assumed. (Naturally, a different electron temperature profile, such as one which possesses a secondary peak in the topside, should not be ruled out as a possible cause of observing this effect in the topside). Since r_{m0} decreases rapidly with sunspot number, we would expect the above behavior to be most frequent during the low sunspot number period of the solar cycle.

Finally, several secondary features originating from the theory due to the magnitude of the separation between N and T_e peaks ($r_{m0} - r_p$) are discussed, but this type of "fine structure" is considered too small to be seen at this time.

ACKNOWLEDGEMENTS

I am grateful for the valuable assistance given to me in the programming and numerical analysis of this work by Christopher E. Bock and William M. Litman. I also offer my deepest thanks to Dr. S. J. Bauer for critically reading the manuscript and making several helpful suggestions.

REFERENCES

Bowles, K. L., Private Communication, 1964.

Brace, L. H., N. W. Spencer and G. R. Carignan, *Ionosphere Electron Temperature Measurements and their Implications*, J. Geophys. Res. **68**, 5397–5412, 1963.

Chandra, S., *Electron Density Distribution in the Upper F Region*, J. Geophys. Res., 68, 1937–1942, 1963.

Chandra, S. and R. A. Goldberg, *Geomagnetic Control of Diffusion in the Upper Atmosphere*, J. Geophys. Res. 69, 3187–3197, 1964.

Croom, S. A. Robbins, and J. O. Thomas, *Two Anomalies in the Behavior of the F2 Layer of the Ionosphere*, Nature **184**, 2003, 1959.

Dalgarno, A., M. F. McElroy and R. J. Moffett, *Electron Temperatures in the Ionosphere*, Planet. Space Sci., **11**, 463–484, 1963.

Evans, J. V., *Diurnal Variation of the Temperature of the F Region*, J. Geophys. Res., **67**, 4914–4920, 1962.

Evans, J. V., *Ionospheric Temperatures during the Launch of NASA Rocket* **8.14** *on July* **2, 1963**, J. Geophys. Res., **69**, 1436–1444, 1964.

Goldberg, R. A. and E. R. Schmerling, *The Distribution of Electrons Near the Magnetic Equator*, J. Geophys. Res., **67**, 3813–3815, 1962.

Goldberg, R. A. and E. R. Schmerling, *The Effect of Diffusion on the Equilibrium Electron Density Distribution in the F Region near the Geomagnetic Equator*, J. Geophys. Res., **68**, 1927–1936, 1963.

Goldberg, R. A., P. C. Kendall and E. R. Schmerling, *Geomagnetic Control of the Electron Density in F the Region of the Ionosphere*, J Geophys. Res. **69**, 417–427, 1964.

Hanson, W. B., *Electron Temperatures in the Upper Atmosphere*, Space Research, Proc. Intern. Space Sci. Symp., 3rd, Washington, 1962, edited by W. Priester

pp. 282–302, North-Holland Publishing Company, Amsterdam, 1962.

HANSON, W. B. and F. S. JOHNSON, *Electron Temperatures in the Ionosphere*, paper presented at Tenth International Astrophysical Colloquium, Liege, Belgium, 1961.

KING, J. W., D. ECCLES, P. A. SMITH, P. DANNAHY, A. LEGG, E. O. OLATUNJI, K. RICE, G. WEBB amd M. WILLIAMS, *Further Studies of the Topside Ionosphere Based on the Topside Sounder Satellite Data*, DSIR Radio Research Station Report No. RRS/I.M. 112 December 1963.

SPENDER, N. W., L. H. BRACE and G. R. CARIGNAN, *Electron Temperature Evidence for Nonthermal Equilibrium in the Ionosphere*, J. Geophys. Res. **67**, 157–175, 1962.

THOMAS, J. O., "The Electron Density Distribution in the F Region of the Ionosphere," in *Electron Density Profiles* edited by B. Maehlum, Pergamon Press, 1962.